SUPPORTING INFORMATION

On-Tip Photodetection: A Simple and Universal Platform for Optoelectronic Screening

Simon Dalgleish[1,2], Louisa Reissig[1,3], Yuki Sudo[3,4,5], Kunio Awaga[1,5]

[1] Department of Chemistry and Research Centre for Material Science, Nagoya University, Furo-cho, Chikusa, 464-8602 Nagoya, Japan

[2] Institute for Advanced Research, Nagoya University, Furo-cho, Chikusa, 464-8601 Nagoya, Japan

[3] Division of Biological Science, Graduate School of Science, Nagoya University, Furo-cho, Chikusa, 464-8602 Nagoya, Japan

[4] Division of Pharmaceutical Sciences, Okayama University, 1-1-1 Tsushima-naka, Kitaku, 700-8530 Okayama, Japan

[5] CREST, JST, Nagoya University, Furo-cho, Chikusa, 464-8602 Nagoya, Japan

EXPERIMENTAL DETAILS

VONPc, C_{60} (99.9%) and P(VDF-HFP) (Mw ~400,000, Mn ~130,000) were purchased from Sigma Aldrich, and EMIM-BF_4 (EB) was purchased at ≥ 98% from Kanto Chemicals. All chemicals were used as received. Detailed discussion of the fabrication and characterization of planar devices of VONPc:C_{60} can be found in our previous publication.[1] The device preparation procedures specific to this study are outlined below:

Protein Expression

The preparation of crude membranes and the purification of *Sr*SRI were performed as previously described.[2,3] In short, proteins with a six-histidine tag at the C-terminus were expressed in *E. coli* BL21 (DE3) cells as recombinant proteins, solubilized by *n*-dodecyl-β-D-maltoside (DDM) and purified using a Ni^{2+} affinity column. The purified proteins were reconstituted into PG liposomes (molar ratio *Sr*SRI:PG 1:50). Bio-Beads (SM-2, Bio-Rad) were used to remove DDM. The samples were stored in the freezer (-20 °C) before use.

Substrate Fabrication

Planar Devices: Devices were prepared on glass slides of dimensions 26 × 18 × 1 mm, pre-cleaned by mild bath ultrasonication (45 W, isopropanol, acetone, chloroform, 10 mins. each). The slides were mounted on a shadow mask, defining electrodes of 2 × 26 mm with 4 mm separation), and inserted into a physical vapor deposition (PVD) apparatus (ULVAC). The chamber was evacuated to an initial vacuum of 4×10^{-4} Pa prior to deposition. Silver (Ag, 200 nm) and gold (Au, 200 nm + 25 nm chromium adhesion layer) electrodes were deposited sequentially at rates of 0.5 $Å s^{-1}$ and 0.2 $Å s^{-1}$ (measured by quartz crystal microbalance (QCM)) for Ag and Cr/Au, respectively, alternately masking one electrode with Kapton tape for each electrode deposition. The substrates were used immediately for active layer deposition without removal from the shadow mask.

On-tip devices: Devices were prepared on pre-cleaned (as above) glass slides of dimensions 26 × 10 × 1 mm. The slides were inserted into a PVD apparatus and coated with gold (Au, 200 nm + 25 nm chromium adhesion layer) at 0.2 $Å s^{-1}$. The substrates were used immediately for active layer deposition.

VONPc:C_{60}: In each case, the active layer was deposited onto the gold electrode at an initial vacuum of 4×10^{-4} Pa using a rotating substrate holder (1 rpm) to improve film homogeneity over the target. VONPc and C_{60} were loaded into adjacent launchers, with their deposition rates monitored independently by different QCMs. The devices were

coupled with a quartz substrate for composition analysis by UV/Vis absorption spectroscopy and thickness analysis by surface profilometry (Dektak 150).

***Sr*SRI:** The PG-reconstituted samples were washed 3× with a 2 mM phosphate buffer (pH 7.0). A droplet of sample of 100 µL, with 4 different protein concentrations (1×, 2×, 4× and 8× diluted) was drop-cast onto a clean Au film on a 1.5 × 3 cm big glass substrate (800 nm Au, Cr adhesion layer). The droplets were dried under reduced pressure, resulting in a homogeneous circular film of a diameter of about 10 mm. The thickness of the samples were measured by profilometry. The films were continuous, however showed a roughness of 1-2 µm (see below). 8 films of four different dilutions were compared. For comparison, 2 films on an ITO substrate were formed and measured for comparison. No major effect of the active electrode could be found.

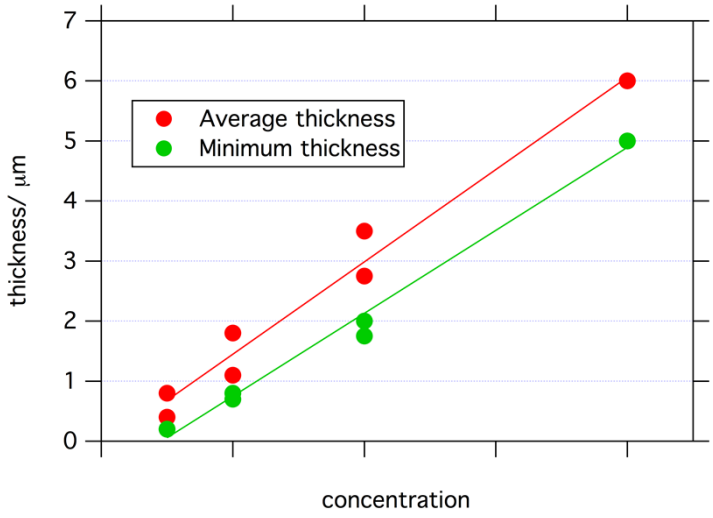

EB:P(VDF-HFP) Gel: Free-standing gel films were prepared by a method similar to Lee *et al.*,[4] using EB in place of ET. In short, a solution of P(VDF-HFP) and EB in acetone (weight ratio 1:4:7, respectively) was drop coated onto a glass slide. The slide was inserted into a vacuum tube and slowly placed under vacuum. The tube was then heated to 70°C overnight, and the gel was stored in a vacuum desiccator until used.

Experimental Setup:

In each case, the device substrate was placed on an xy translating stage, and held in place with gold pad(s) connected to the electrode(s). For the planar devices, the gold working electrode was connected to the input of the amplifier, and the silver counter electrode grounded to the amplifier. For on-tip devices, the steel SMA tip of the fiber was secured to a steel female mounting ring, grounded to the amplifier, and was positioned using a z-axis translating stage.

Device Testing:

The time-dependent transient photocurrent measurements were performed using a 1 mm core fiber-coupled LED light source (VONPc:C_{60}: λ_{MAX} = 850 nm, $P_{MAX,total}$ = 700 µW;

SrSRI: λ_{MAX} = 530 nm, $P_{MAX,total}$ = 1.16 mW), powered by a home-built driver circuit (circuit diagram available upon request), and modulated by a function generator (Tektronix AFG320). The devices were connected to a non-inverting transimpedance amplifier (Femto DLPCA-200) in which the transient short circuit current signal was amplified and converted into a voltage signal, which was visualized by an oscilloscope (Tektronix TDS5104B). The light power density was determined before each dataset using an optical power meter (ADCMT, 8230E). For convention, all data was not inverted, *i.e.* a positive peak corresponds to holes being extracted from the active layer at the gold electrode, and the first peak in a photocurrent plot corresponds to light on.

ESI FIGURE LEGENDS

FIGURE S1: Sketch of a generalized MISM device under illumination.

FIGURE S2: Comparison of the waveforms of pure ionic liquid (EB) and ionic gel (EB:PVDF-HFP) in an on-tip device. The different shape of the waveforms (in contrast to Manuscript Fig. 1) is due to the different electrode separations, since to make contact with the gel, the fiber tip was lowered to <1mm above the working electrode.

FIGURE S3: Non-normalized waveforms for on-tip measurement of VONPc:C_{60} films (a) upon repeated dipping into a drop of EB, and (b) between drops of EB. Between (a) and (b) the area of the IL/tip contact was increased by rolling an additional drop of IL down the shaft of the ferrule, thereby increasing the volume of the drop that the fiber was inserted into, and thereby its contact area. Due to favorable wetting of the ferrule, the new contacting area could be maintained when the tip was inserted into subsequent drops, as the IL wetting the shaft did not appreciably diminish upon removal from the drop.

FIGURE S4: Dependence of power density on tip height for fiber-coupled LED (530nm) used in this study.

FIGURE S5: Comparison of the waveforms of different electrolyte solutions used for on-tip detection.

FIGURE S6: UV-Vis absorption spectrum of *Sr*SRI in PG liposomes in the absence and presence of NaCl, recorded by a UV2450 spectrophotometer with an ISR2200 integrating sphere (Shimazu, Kyoto, Japan) at 25°C. Upon addition of NaCl, a redshift of the absorption maximum can be seen. The green line represents the LED light used in photocurrent experiments.

ESI FIGURE S1

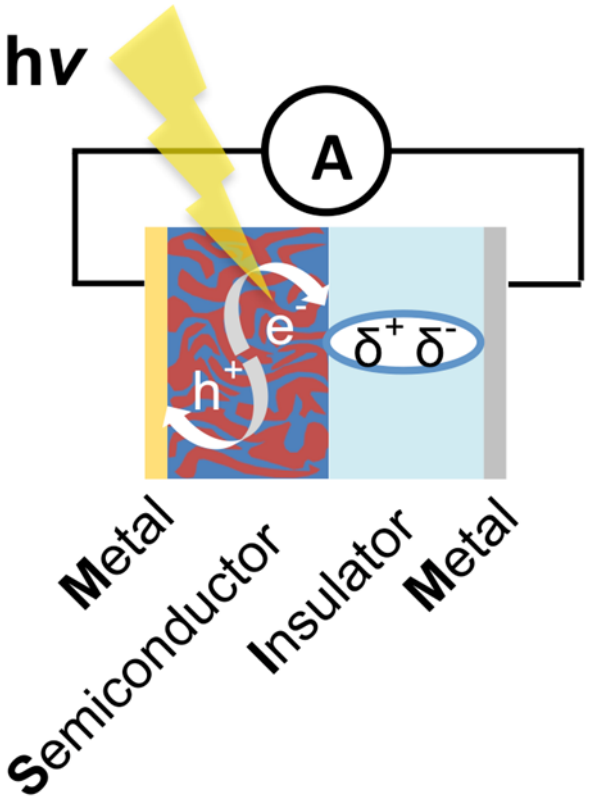

ESI FIGURE S2

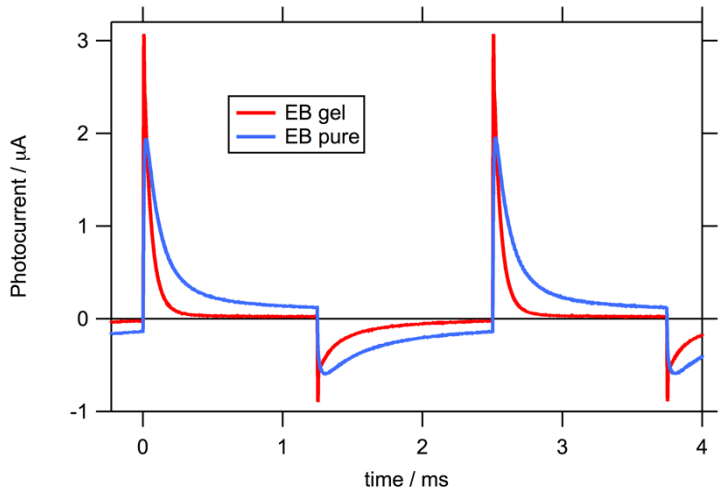

ESI FIGURE S3

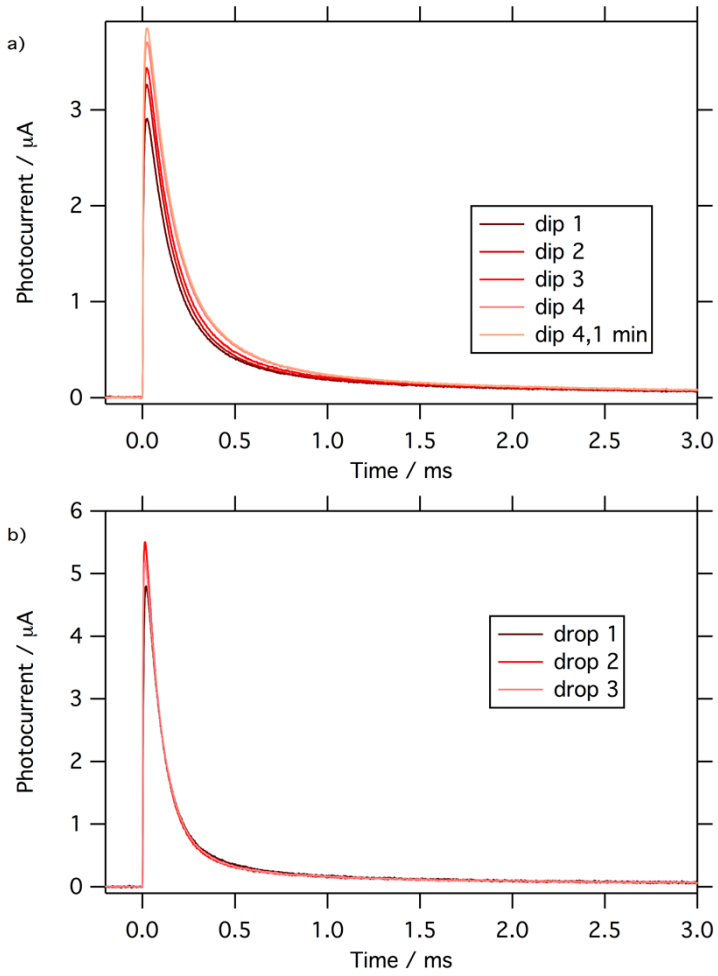

ESI FIGURE S4

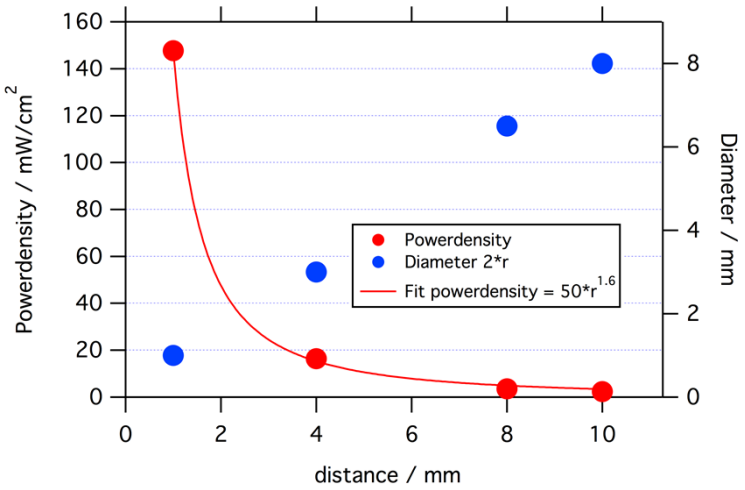

ESI FIGURE S5

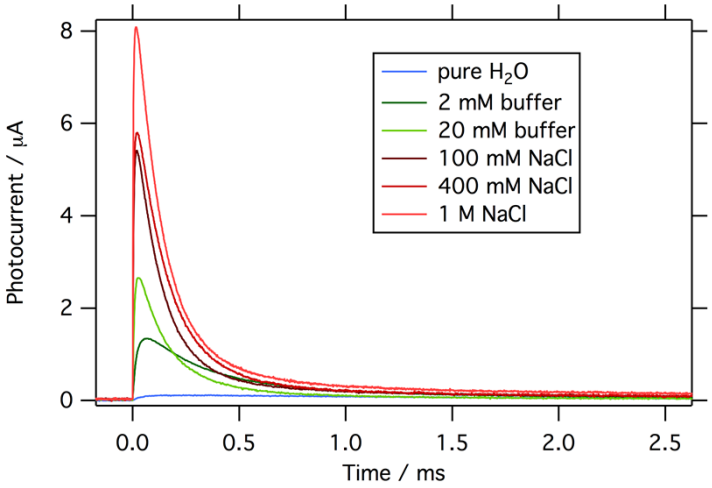

ESI FIGURE S6

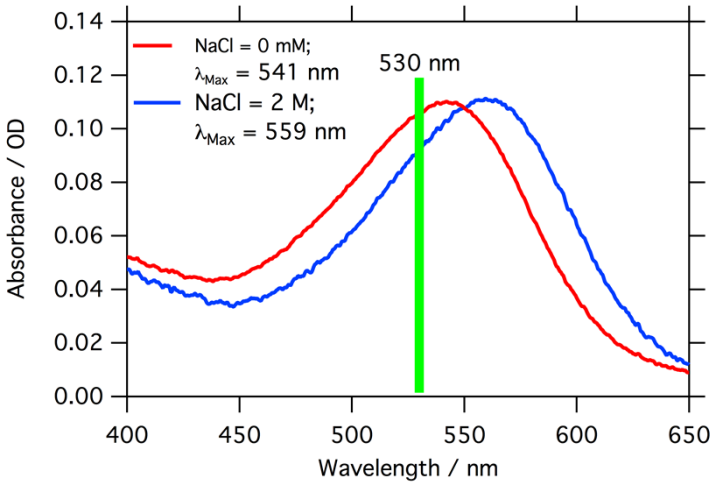

1. Dalgleish, S.; Reissig, L.; Hu, L.; Matsushita, M. M.; Sudo, Y.; Awaga, K. Factors affecting the stability and performance of ionic liquid-based planar transient photodetectors. *Langmuir* **2015**, *31*, 5235–5243.
2. Sudo, Y., Okada, A., Suzuki, D., Inoue, K., Irieda, H., Sakai, M., Fujii, M., Furutani, Y., Kandori, H., Homma, M. Characterisation of a signalling complex composed of sensory rhodopsin I and its cognate transducer protein from the eubacterium Salinibacter ruber. *Biochemistry* **2009,** *48*, 10136-10145
3. Reissig, L.; Iwata, T.; Kikukawa, T.; Demura, M.; Kamo, N.; Kandori, H.; Sudo, Y. Influence of Halide Binding on the Hydrogen Bonding Network in the Active Site of Salinibacter Sensory Rhodopsin I. *Biochemistry* **2012**, *51*, 8802-8813
4. Lee, K. H.; Kang, M. S.; Zhang, S.; Gu Y.; Lodge, T. P.; Frisbie, C. D. "Cut and Stick" Rubbery Ion Gels as High Capacitance Gate Dielectrics. *Adv. Mater*. **2012**, *24*, 4457–4462